Electronic Supplementary Material (ESI) for Journal of Materials Chemistry C.

Excitation dependent multicolour luminescence and colour blue-shifted afterglow at room-temperature of europium incorporated hydrogen-bonded multicomponent frameworks

Chaoqing Yang,[a] Flavia Artizzu, [a]* Karel Folens,[b] Gijs Du Laing,[b] and Rik Van Deun[a] *

[a] Department of Chemistry, Ghent University, Krijgslaan 281-S3, B-9000 Ghent, Belgium

[b] Department of Green Chemistry and Technology, Ghent University, Coupure Links 653, B-9000 Ghent, Belgium

Supplementary experimental section

1.1 Synthesis of melamine-isophthalic acid-trimesic acid hydrogen-bonded organic framework (MIT)

0.101 g (0.8 mmol) of melamine and 0.053 g (0.25 mmol) of trimesic acid were separately dissolved in 15 mL of deionized water under stirring at 95 °C. 0.083 g (0.5 mmol) of isophthalic acid were dissolved in 25 mL of deionized water under stirring at 100 °C. Next, the isophthalic acid and the trimesic acid solutions were successively added to the dissolved melamine solution under stirring, and a white solid precipitated immediately. The mixture was cooled down to room temperature then centrifuged and washed with deionized water. The precipitate was dried in an oven at 40 °C, 85 °C, 130 °C, and 175 °C. The obtained samples were labeled as MIT-40, MIT-85, MIT-130, and MIT-175, respectively.

1.2 Synthesis of Eu^{3+}-doped melamine-isophthalic acid-trimesic acid hydrogen-bonded organic framework (MIT:Eu)

For the Eu^{3+}-doped MIT, 0.101 g (0.8 mmol) of melamine and 0.053 g (0.25 mmol) of trimesic acid were separately dissolved in 15 mL of deionized water under stirring at 95 °C. 0.083 g (0.5 mmol) of isophthalic acid was dissolved in 25 mL of deionized water under stirring at 100 °C. Then 0.062 mL (0.1 mol/L) of europium nitrate solution was added to the melamine solution. Next, the isophthalic acid and the trimesic acid solution were successively added to the melamine and Eu^{3+} solution under stirring, and a white solid precipitated immediately. The mixture was cooled down to room temperature, then centrifuged and washed with deionized water. The precipitate was dried in an oven at 40 °C, 85 °C, 130 °C, and 175 °C and the obtained samples were labeled as MIT:1Eu-40, MIT:1Eu-85, MIT:1Eu-130, and MIT:1Eu-175, respectively. Other samples with different molar ratios of MIT to europium, in 130:1, 70:1, and 40:1 ratios were also synthetized. The samples were labelled as MIT:2Eu, MIT:3Eu, and MIT:4Eu, respectively. A summary of the actual Eu^{3+} concentrations found for the MIT:Eu samples by ICP-MS (inductively coupled plasma mass spectrometry) is presented in Table S2.

1.3 Synthesis of melamine-isophthalic acid hydrogen-bonded organic framework (MIP)

The melamine isophthalic acid (MIP) hydrogen-bonded organic framework was synthesized by referring to a previous report.[1] 0.063 g (0.5 mmol) of melamine, 0.083 g (0.5 mmol) of isophthalic acid, and 20 ml deionized water were put into a two-necked round bottom flask. After being heated in an oil bath at 150 °C for 10 min, the turbid solution got clear. The mixture was then cooled at a rate of 20 °C h^{-1} to ambient temperature, and colorless crystals were obtained. The crystals were centrifuged and washed with water. The sample was dried in an oven at 40 °C. For the Eu^{3+} -doped MIP (MIP:Eu), the same procedure as above was used, except for the addition of 0.1 mL (0.1 mol/L) of an europium nitrate water solution.

1.4 Synthesis of Eu^{3+} coordinated trimesic acid complex (TMA:Eu)

The TMA:Eu complex was synthesized by referring to a previous report.[2] 1.5 g (7.5 mmol) of trimesic acid was dissolved in 250 mL of distilled water. The pH was then adjusted to 6.0 by adding dropwise NaOH 0.1 mol L^{-1}. An equimolar (7.5 mmol) europium nitrate solution was dropwise added to the mixture under stirring. A few minutes after the beginning of the process, a starting white precipitation was observed. In order to increase the yield, the resulting reaction mixture was refluxed for 2 h. The precipitate was filtered, washed with hot water several times and dried at 130 °C.

1.5 Synthesis of Eu^{3+} coordinated isophthalic acid complex (IPA:Eu)

The IPA:Eu complexes was synthesized by referring to a previous report.[3] In a typical reaction, 0.83 g (5 mmol) of trimesic acid were dissolved in 100 mL of distilled water. The pH was adjusted to 6.0 by adding dropwise NaOH 0.1 mol L^{-1}. An equimolar (5 mmol) europium nitrate solution was dropwise added to the mixture under stirring. A few minutes after the beginning of the process, a starting white precipitate was observed. In order to increase the yield, the resulting reaction mixture was refluxed for 2 h. The precipitate was filtered, washed with hot water several times and dried at 130 °C.

1.6 Synthesis of Eu^{3+} coordinated melamine complex (Mel:Eu)

The Mel:Eu complexes was synthesized by referring to a previous report.[4] In a typical reaction, europium nitrate (0.5 mmol) was stirred with melamine (0.5 mmol) in a 1:1 mixed solvent (30 ml) of methanol and water for 7 days. The precipitate was filtered and dried at 130 °C.

Supplementary figures and tables

Table S1. Organic elemental (N, C, and H) analysis of investigated samples.

Sample	N (wt %)	C (wt %)	H (wt %)	N/C
MIT $^{(calcd)}$	28.43	43.93	3.94	0.65
MIT-130	27.37	43.57	3.89	0.63
MIT:1Eu-130	26.41	43.37	3.83	0.61
MIT:2Eu-130	25.71	43.40	3.77	0.59
MIT:3Eu-130	23.36	42.64	3.63	0.55
MIT:4Eu-130	23.33	41.72	3.45	0.56

Table S2. Actual europium contents for the investigated samples determined by ICP-MS analysis.

Sample	concentration
MIT:1Eu-130	0.29%
MIT:2Eu-130	0.53%
MIT:3Eu-130	1.11%
MIT:4Eu-130	1.79%

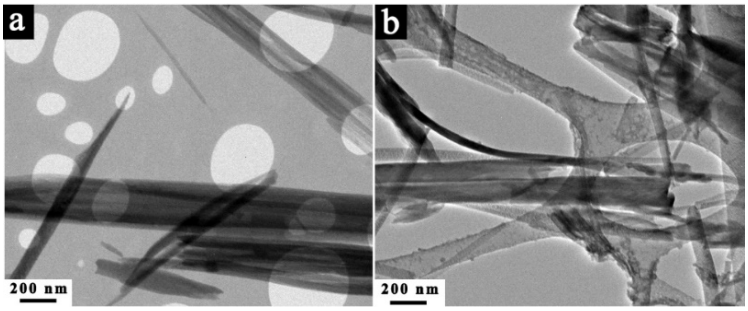

Figure S1. TEM images of (a) for MIT:3Eu and (b) for MIT:4Eu.

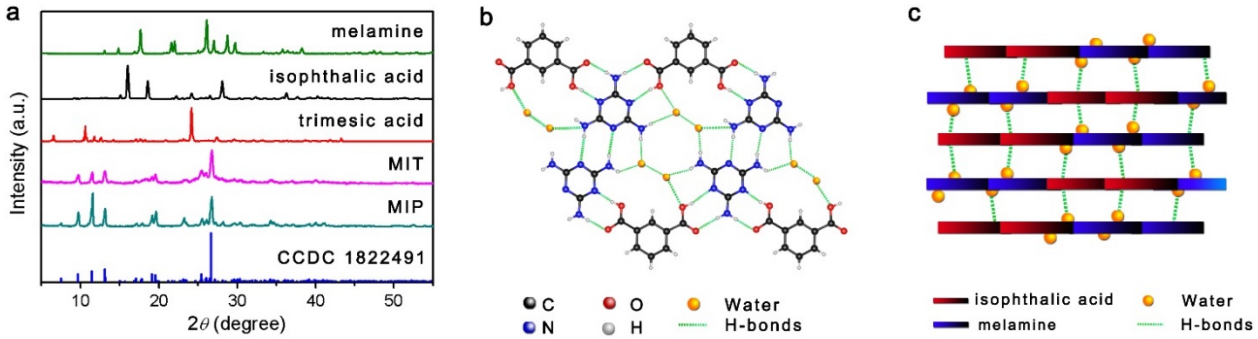

Figure S2. (a) Normalized PXRD patterns of melamine, trimesic acid, isophthalic acid, as-prepared MIT-40, and as-prepared MIP. The vertical blue bars at the bottom are the positions of reported single crystal MIP (CCDC 1822491).[1] (b) Molecular packing of melamine and isophthalic acid in a single layer of crystal MIP. (c) Intermolecular interactions of different layers in the crystal MIP.

The MIP hydrogen-bonded material has been reported by Huang et al.[1] The isophthalic acid has only two carboxylic acids as H-bonds acceptors, while the melamine has three H-bonds donors. Several molecules of water are captured by multiple short and intense H-bonds in order to construct the MIP network. The trimesic acid has a similar structure and size as isophthalic acid but three carboxylic acid groups as H-bonds acceptors. In our synthesis route, the isophthalic acid in MIP framework was partly replaced by trimesic acid. As shown in **Figure S2a**. The powder X-ray diffraction (PXRD) pattern of the as-synthesized MIP is consistent with the single crystal data. Three well-resolved peaks at lower angles, 9.76, 11.59, and 13.11, are attributed to the in-planar packing between melamine, isophthalic acid, and water molecules through multiple H-bonds, N−H···O and N−H···N (**Figure S2b**). Another strong broad peak at 26.81°, corresponding to a *d*-spacing of 0.331 nm supports the π-π stacking of individual MIP nanolayers as shown in **Figure S2c**. As expected, the as-synthesized MIT framework demostrates a very similar XRD pattern as the MIP. It is possible to propose that the MIT framework might have an analogous molecular packing and layered structure as the MIP framework, which is partly confirmed by the TEM images shown in **Figure 1**. Additionally, no characteristic peaks of impurities are found in as-prepared MIT framework.

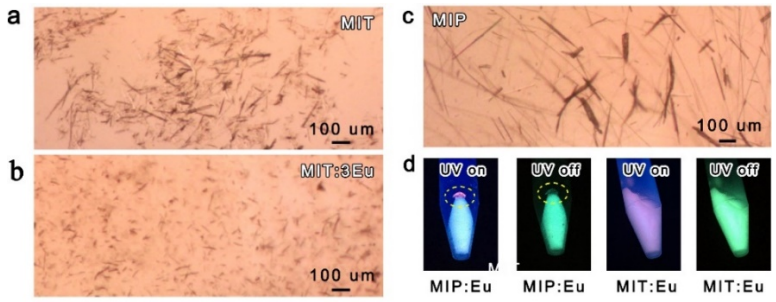

Figure S3. Optical microscope image of micron-sized (a) MIT, (b) MIT:3Eu, and (c) MIP on glass slides. (d) The luminescence images of MIP:Eu and MIT:Eu in a centrifuge tube taken during and after UV illumination (302 nm).

The optical microscope images of the as-synthesized MIT shown in **Figure S3a** displays many unequal-sized colorless acicular crystals with a length up to hundreds microns. These acicular crystals have a diameter up to a few microns. The Eu doped MIT crystals (**Figure S3b**) are of a smaller size. The as-synthesized MIP is also shown in **Figure S3c** as reference. The MIP show many differently sized acicular crystals as MIT. We also attempted the synthesis of Eu-doped MIP HOFs (MIP:Eu). As shown in **Figure S3d**, the luminescence images of MIP:Eu in a centrifuge tube indicate an inhomogenous composition with a small spot emitting red/pink light, whereas MIT:Eu yields homogeneously pink fluorescence under 302 nm illumination. Moreover, the region of red fluorescence in MIP:Eu also does not show obvious and homogeneous green afterglow like MIT:Eu after switching off the irradiation source. This might indicate that MIP framework can not effectively host Eu ions as the MIT framework. Although both trimesic acid and isophthalic acid can be used as organic ligands for Ln ions, the trimesic and isophthalic acid have different coordination ability and bonding modes with trivalent rare earth ions.[2, 3]

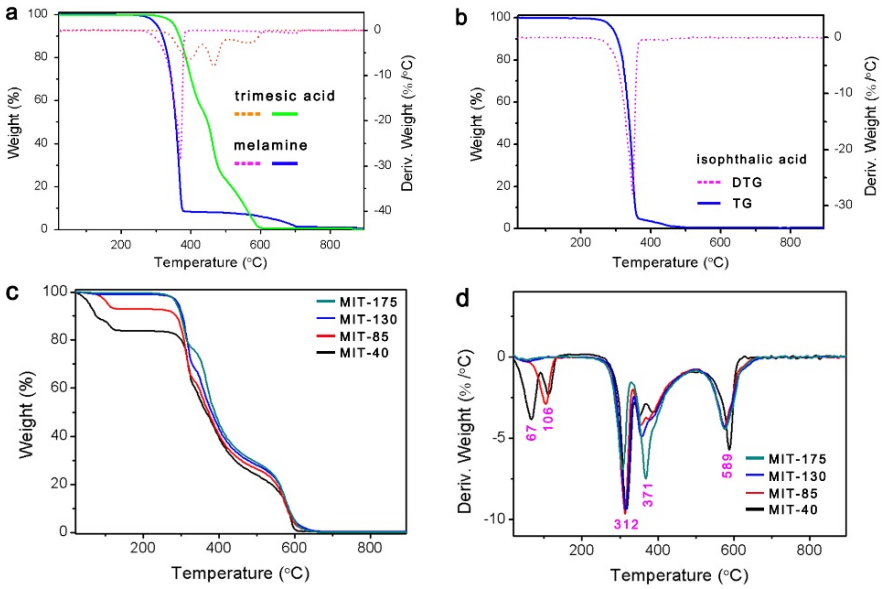

Figure S4. (a) TG and DTG curves of trimesic acid and melamine. (b) TG and DTG curves of isophthalic acid. (c) TG curves of as-prepared MIT after drying at different temperatures. (d) DTG curves of the as-prepared MIT dried at different temperatures.

TG (thermogravimetry) and DTG (derivative thermogravimetry) are used to investigate the structure evolution of the as-synthesized materials with the rising temperature. As shown in **Figure S4a** and **S4b**, the

melamine and isophthalic acid begin to break down quickly at temperatures higher than 350 °C, and the decompositions are almost completed before 400 °C. Trimesic acid has a better thermal stability in the temperature range of 400-550 °C. The weight loss of the three materials at higher temperatures over 550 °C is attributed to the combustion of the benzene ring or triazine skeleton. The TG and DTG curves of MIT were recorded in the temperature interval from 20 to 860 °C. As shown in **Figure S4c** and **S4d**, the TG and DTG curves clearly show the different content and type of water in these investigated MIT samples due to the different treatment process. The TG curve of MIT-40 shows two small weight loss steps in the range of 20 – 250 °C attributed to the release of free and bound water molecules. Another large mass loss in the temperature range of 250-850 °C should be attributed to the decomposition of organic components. With the aid of the first derivative of TG curve, it is possible to distinguish the two processes of water losses. The first DTG peak at 67 °C should correspond to free water molecules which weakly interact with the matrix. More strongly linked water molecules, identified as bound water, give rise to a second DTG peak at 109 °C.[5] The DTG curve of MIT-85 only has one obvious peak at 106 °C in the temperature range of 20-250 °C whereas there is no apparent DTG peak for the MIT-130 and the MIT-175 in the same range. The actual water contents for the investigated samples are given in **Table S3**.

Table S3. Actual water contents for the investigated samples determined by TG analysis.

Sample	Water concentration (wt%)	Sample	Water concentration (wt%)
MIT-40	16.42	MIT:3Eu-40	20.61
MIT-85	6.57	MIT:3Eu-85	8.01
MIT-130	1.25	MIT:3Eu-130	1.38
MIT-175	0.39	MIT:3Eu-175	0.44

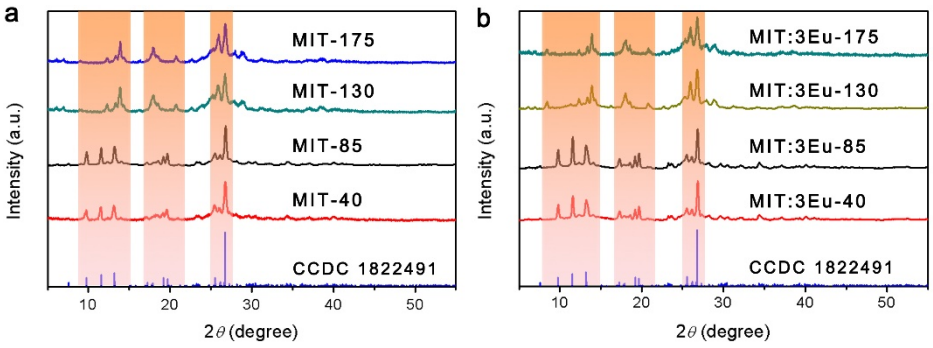

Figure S5. Normalized PXRD patterns of the as-prepared (a) MIT and (b) MIT:3Eu after drying at 40 °C, 85 °C, 130 °C, and 175 °C. The vertical blue bars at the bottom are the positions of reported single crystal MIP (CCDC 1822491).

Normalized PXRD patterns of the as-prepared MIT (**Figure S5a**) after drying at different temperatures demonstrates the structure transitions originating from the loss of bound water. MIT-40 and MIT-85 present the same XRD pattern as the reported single crystal MIP.[1] As the MIT samples undergo a thermal treatment at a temperatures over 120 °C, the PXRD patterns of MIT-130 and MIT-175 show significant changes. These dehydrated MIT samples show very similar diffraction peaks as the reported dehydrated MIP, which further confirm that the as-prepared MIT HOFs have similar molecular packing and layered structure as the MIP framework. The normalized PXRD patterns of MIT:Eu shown in **Figure S5b** are in accordance with the structure analysis of MIT.

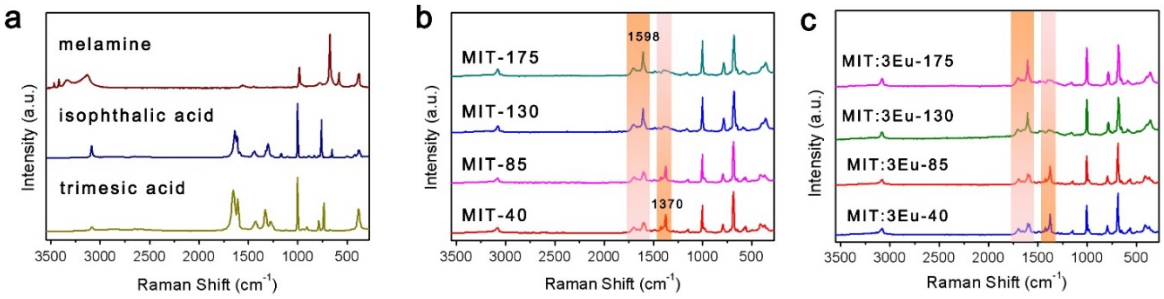

Figure S6. (a) Normalized FT-Raman spectra of trimesic acid, isophthalic acid, and melamine. Normalized FT-Raman spectra of the as-prepared (b) MIT and (c) MIT:3Eu after drying at 40 °C, 85 °C, 130 °C, and 175 °C.

Fourier transform Raman spectroscopy (FT-Raman) is used to investigate the structure evolution of the as-synthesized materials with the rising temperature. Melamine showed the characteristic Raman vibration bands of the triazine ring at 675 and 983 cm^{-1}. The double peaks at 3489 and 3426 cm^{-1} are ascribed to the $-NH_x$ groups. The most significant Raman vibration modes observed in trimesic acid are O=C-O and C-O-H stretching vibrations, benzene ring breathing vibration, symmetric stretching vibration of C=O, C-O-H asymmetric stretching vibration, O-C=O wagging vibration, COOH out-of-plane vibration and C-C symmetric stretching modes. Isophthalic acid displays similar Raman vibration modes as trimesic acid due to a similar structure. The FT-Raman spectrum of MIT-40 shows a series of vibration peaks. The peak at 682 cm^{-1} is ascribed to the vibration mode of the triazine ring, and the peaks at 786 and 1004 cm^{-1} are attributed to the stretching vibrations of the benzene ring. Few weak peaks at 1600 cm^{-1} are originating from the carboxylic acids groups. The structure change of dehydrated MIT originating from the loss of bound water is further confirmed by FT-Raman spectroscopy shown in **Figure S6b**. A Raman peak of the hydrated MIT at 1370 cm^{-1} belonging to the stretching vibration of the H-bonded ring of TMA with water obviously weakens in dehydrated MIT. The dehydrated MIT presents a stronger Raman peak at 1598 cm^{-1} attributed to the characteristic stretching vibrational modes of C=O, which might originate from the destruction of O−H···O hydrogen bonds after dehydrating.[6] The normalized FT-Raman spectra of MIT:Eu shown in **Figure S6c** are in accordance with the FT-Raman analysis of MIT.

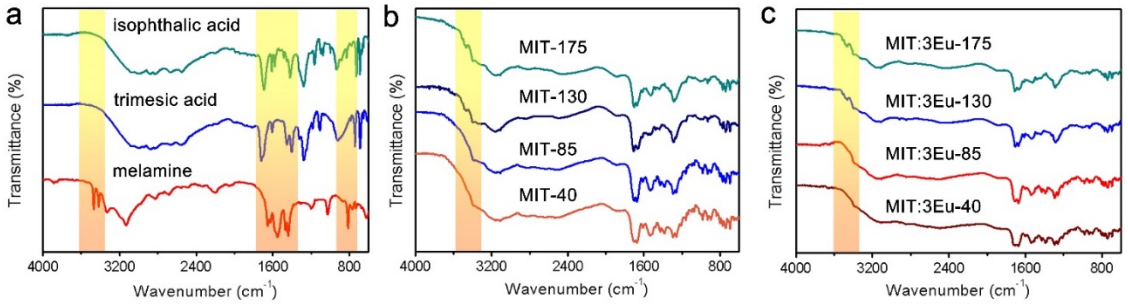

Figure S7. (a) Normalized DRIFTS spectra of trimesic acid, isophthalic acid, and melamine. Normalized DRIFTS spectra of the as-prepared (b) MIT and (c) MIT:3Eu after drying at 40 °C, 85 °C, 130 °C, and 175 °C.

Moreover, the structure changes of dehydrated MIT are further confirmed by diffuse reflectance infrared fourier transform spectroscopy (DRIFTS). As shown in **Figure S7a**, melamine displays a sharp absorption peak at 810 cm^{-1} assigned to the breathing mode of triazine units. Several peaks from 1238 to 1640 cm^{-1} dominate the spectra, corresponding to the characteristic stretching modes of C−N heterocycles. Several broad and sharp peaks in the range of 3000–3700 cm^{-1} are attributed to the N−H stretching of amino groups. Trimesic acid exhibits C=O, O–H, and C–O stretching vibrations at 1728, 1455 and 1286 cm^{-1}, respectively, originating from the aromatic acid.[7] The absorption at 755 cm^{-1} can be attributed to the C–H deformation vibration of the aromatic ring. Isophthalic acid shows a similar DRIFTS spectrum as trimesic acid due to a similar structure. The formation of H-bonds in the hydrated MIT materials can be clearly evidenced by DRIFTS

spectroscopy (**Figure S7b** and **S7c**). Two sharp absorption peaks at 3487 and 3423 cm^{-1} attributed to the stretching vibrations of free N−H disappear for the hydrated MIT, which should indicate the occurrence of N−H···O hydrogen bonds between the MIT matrix and water molecules.

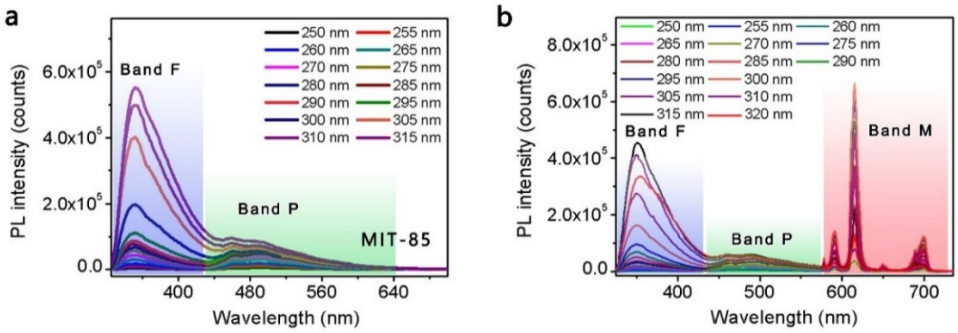

Figure S8. Steady-state emission spectra of (a) MIT-85 and (b) MIT:3Eu-85 powder following different excitation wavelengths under ambient conditions. The colourful shadows show the three main emission bands: Band F, Band P, and Band M.

Table S4. CIE chromaticity coordinates for MIT-85 following different excitation wavelengths.

wavelength	CIE coordinates (x, y)	wavelength	CIE coordinates (x, y)
250	(0.209, 0.342)	285	(0.206, 0.320)
255	(0.210, 0.341)	290	(0.207, 0.314)
260	(0.208, 0.334)	295	(0.208, 0.306)
265	(0.206, 0.333)	300	(0.203, 0.271)
270	(0.206, 0.328)	305	(0.192, 0.223)
275	(0.206, 0.320)	310	(0.191, 0.220)
280	(0.205, 0.320)	315	(0.190, 0.212)

Table S5. CIE chromaticity coordinates for MIT:3Eu-85 following different excitation wavelengths.

wavelength	CIE coordinates (x, y)	wavelength	CIE coordinates (x, y)
250	(0.508, 0.339)	290	(0.471, 0.338)
255	(0.500, 0.340)	295	(0.479, 0.337)
260	(0.482, 0.341)	300	(0.481, 0.328)
265	(0.465, 0.336)	305	(0.432, 0.307)
270	(0.464, 0.344)	310	(0.347, 0.287)
275	(0.455, 0.340)	315	(0.288, 0.260)
280	(0.469, 0.339)	320	(0.257, 0.245)
285	(0.476, 0.338)		

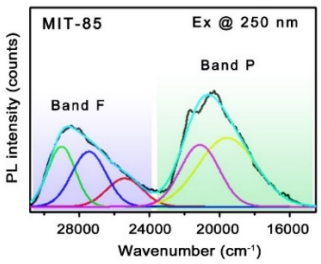

Figure S9. Deconvoluted steady-state emission spectra of MIT-85 under excitation at 250 nm.

Table S6: Gaussian fitting results of steady-state emission spectra of MIT-85 and MIT:3Eu-85.

Samples	Excitation wavelength	Band F			Band P	
		F 1	F 2	F 3	P 1	P 2
MIT-85	250 nm	28992 cm^{-1}	27431 cm^{-1}	25390 cm^{-1}	21252 cm^{-1}	19549 cm^{-1}
MIT:3Eu-85	250 nm	28692 cm^{-1}	27227 cm^{-1}	25076 cm^{-1}	21112 cm^{-1}	19156 cm^{-1}

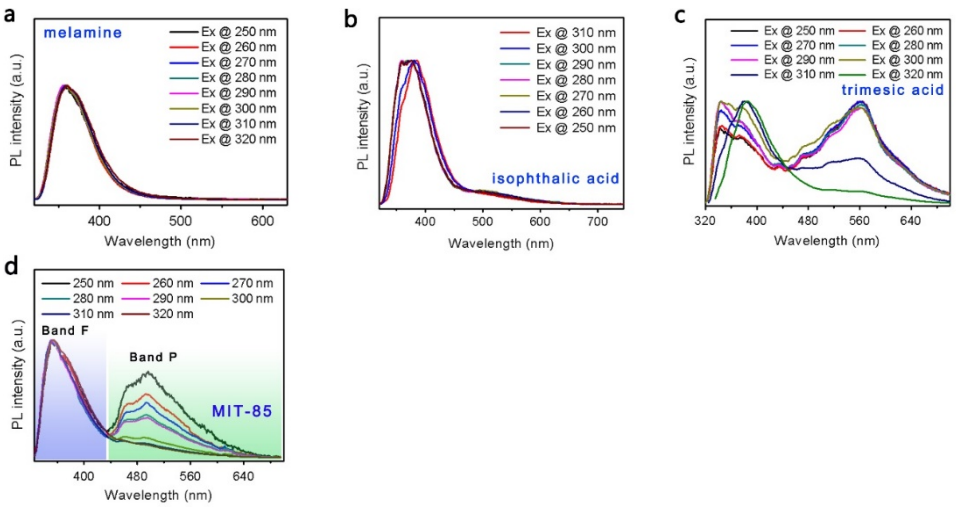

Figure S10. Normalized steady-state emission spectra of (a) melamine, (b) isophthalic acid, (c) trimesic acid, and (d) MIT-85 following different excitation wavelengths under ambient conditions. The spectra of MIT-85 were normalized to the intensity of band F at 355 nm.

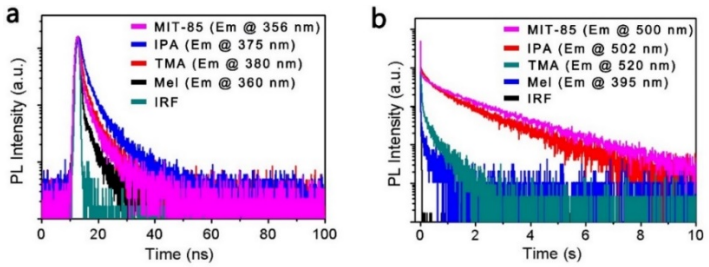

Figure S11. (a) and (b) luminescence decay profiles of MIT-85, melamine, isophthalic acid, and trimesic acid under ambient conditions. The instrument response function (IRF) curves are also shown.

Table S7: Fitting results of the luminescence decay curves of the investigated samples.

Samples	Emission wavelength (nm)	A (%)	τ (ns)	R^2
MIT-85	356	100	3.16	0.971
melamine	360	100	2.96	0.949
isophthalic acid	375	100	3.92	0.984
trimesic acid	380	100	3.47	0.955

Table S8: Fitting results of the luminescence decay curves of the investigated samples.

Samples	Emission wavelength (nm)	τ_1 (s)	A_1 (%)	τ_2 (s)	A_2 (%)	τ_{ave} (s)	R^2
MIT-85	500	0.288	38.3	1.677	61.7	1.543	0.996
melamine	395	0.013	90.1	0.165	9.9	0.102	0.928
isophthalic acid	502	0.247	57.1	1.331	42.9	1.116	0.995
trimesic acid	520	0.065	72.6	0.385	27.4	0.286	0.973

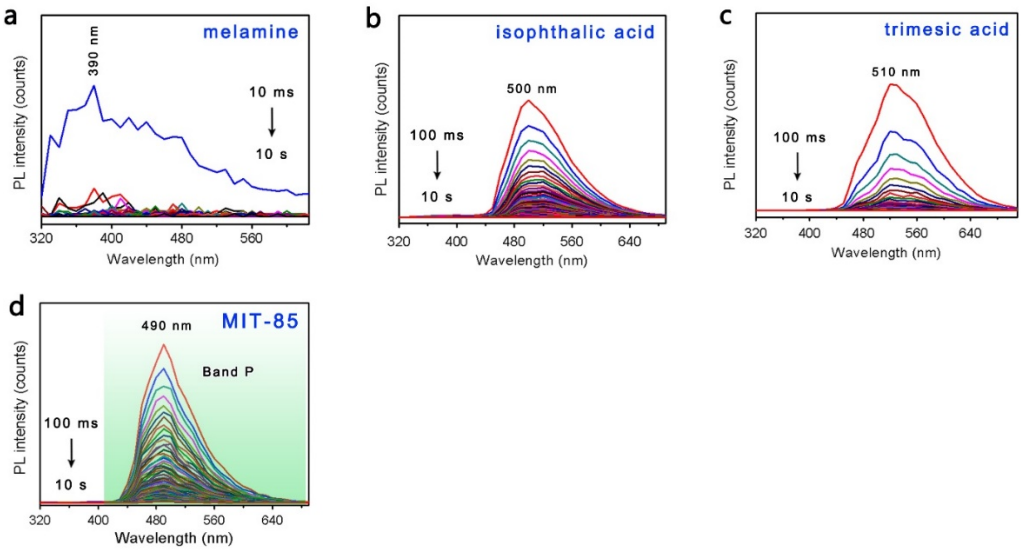

Figure S12. Sliced time-resolved emission spectra of (a) melamine, (b) isophthalic acid, (c) trimesic acid, and (d) MIT-85 following excitation at 300 nm under ambient conditions.

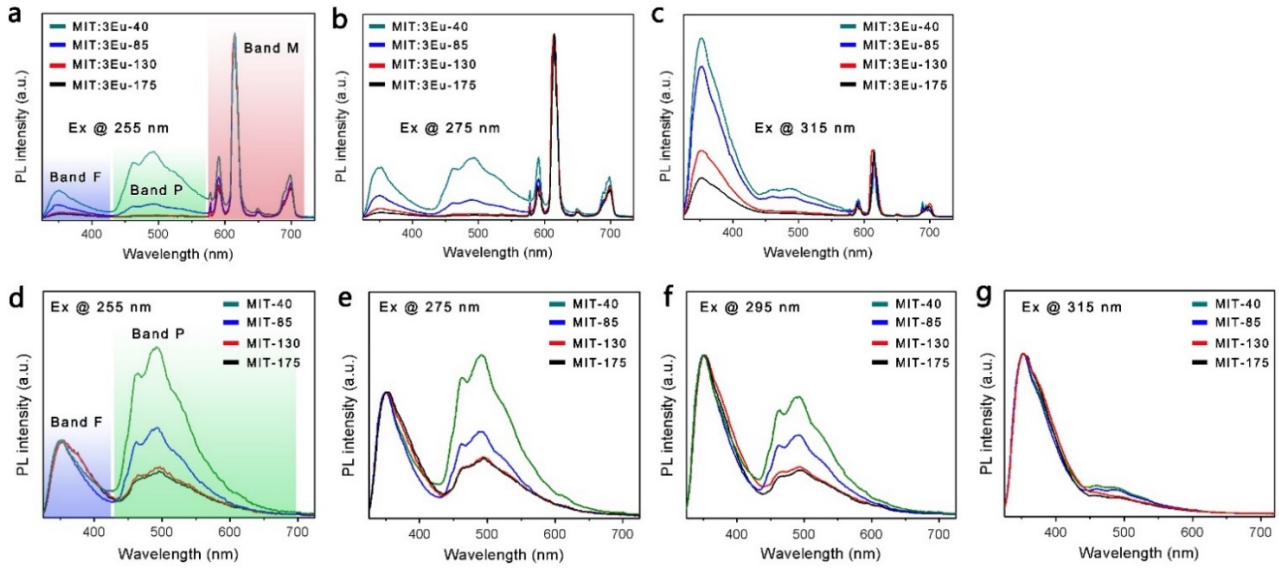

Figure S13. Normalized steady-state emission spectra of MIT:3Eu samples excited at (a) 255 nm, (b) 275 nm, and (c) 315 nm under ambient conditions. The colourful shadows indicate the three main emission bands, F, P and M. The spectra were normalized to the intensity of band M at 614 nm. Normalized steady-state emission spectra of MIT samples following excitation wavelengths at (d) 255 nm, (e) 275 nm, (f) 295 nm, and (g) 315 nm under ambient conditions. The spectra were normalized to the intensity of band F at 355 nm.

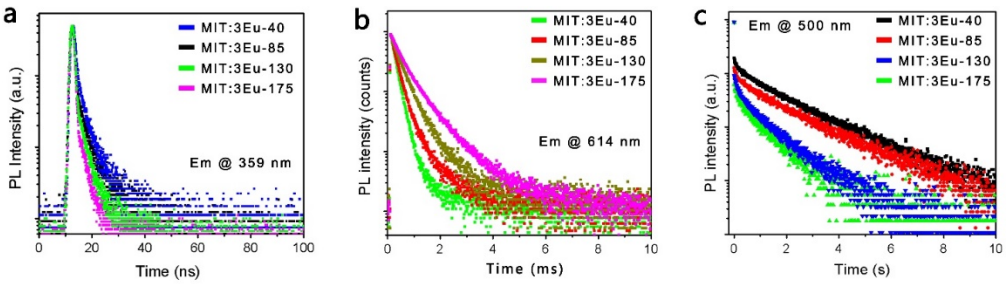

Figure S14. Luminescence decay profiles of MIT:3Eu samples monitored at (a) 359 nm, (b) 614 nm, and (c) 500 nm under ambient conditions.

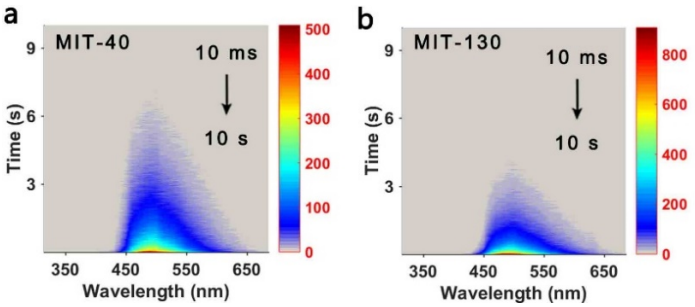

Figure S15. Time-resolved emission mapping of (a) MIT-40 and (b) MIT-130 excited at 300 nm under ambient conditions in the time range from 10 ms to 10 s. The color bar changing red to gray indicates the decrease in emission intensity.

Table S9. Fitting results of the luminescence decay curves of MIT:3Eu under ambient conditions.

Samples	Emission wavelength (nm)	*A* (%)	τ (ns)	τ (us)	τ (s)	R^2
MIT:3Eu-40	359	100	3.25	-	-	0.970
MIT:3Eu-85	359	100	3.18	-	-	0.977
MIT:3Eu-130	359	100	2.76	-	-	0.972
MIT:3Eu-175	359	100	2.71	-	-	0.981
MIT:3Eu-40	614	100	-	0.206	-	0.997
MIT:3Eu-85	614	100	-	0.288	-	0.994
MIT:3Eu-130	614	100	-	0.422	-	0.997
MIT:3Eu-175	614	100	-	0.577	-	0.998
MIT:3Eu-40	500	100	-	-	1.45	0.993
MIT:3Eu-85	500	100	-	-	1.43	0.989
MIT:3Eu-130	500	100	-	-	0.79	0.979
MIT:3Eu-175	500	100	-	-	0.77	0.984

Quantum yield measurements

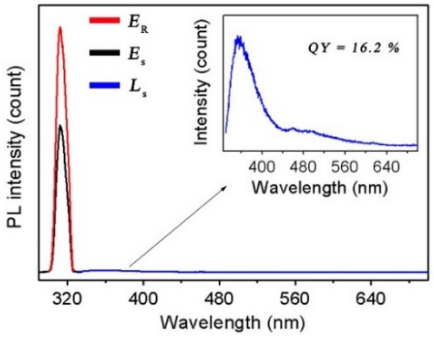

Figure S16. Quantitative luminescence spectra of MIT-85 powder and reference sample measured using an integrating sphere. The inset shows a magnification of the emission spectrum of MIT-85 powder.

The internal quantum efficiencies were measured using an integrating sphere on the FLSP920 instrument, and white $BaSO_4$ powder was used as a reference to measure the scattered excitation light. The internal (η_i) quantum efficiencies (*QEs*) were calculated by using the following equation,[8]

$$\eta_{\mathrm{i}} = \frac{\varepsilon}{\alpha} = \frac{\int L_S}{\int E_R - \int E_S}$$

where ε is the number of photons emitted by the sample and α is the number of photons absorbed by the sample. L_S is the luminescence emission spectrum of the sample; E_R is the spectrum of the scattered excitation light with the $BaSO_4$ reference sample in the sphere; E_S is the spectrum of the scattered excitation light with the actual sample in the sphere; all spectra were collected using the sphere. The quantum efficiencies of the other samples were measured using the same method and setup.

Table S10. Photoluminescence efficiency (*Φ*) of investigated MIT and MIT:3Eu materials.

Sample	quantum yields (%)
MIT:3Eu-40	10.3
MIT:3Eu-85	9.1
MIT-85	16.2
MIT:3Eu-130	5.4
MIT:3Eu-175	4.1

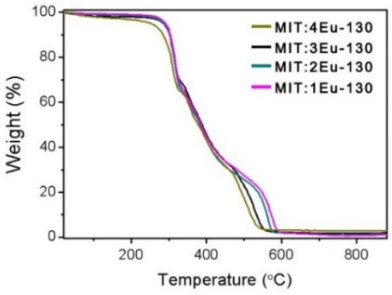

Figure S17. TG curves of the as-prepared dehydrated MIT:Eu-130 with different europium contents.

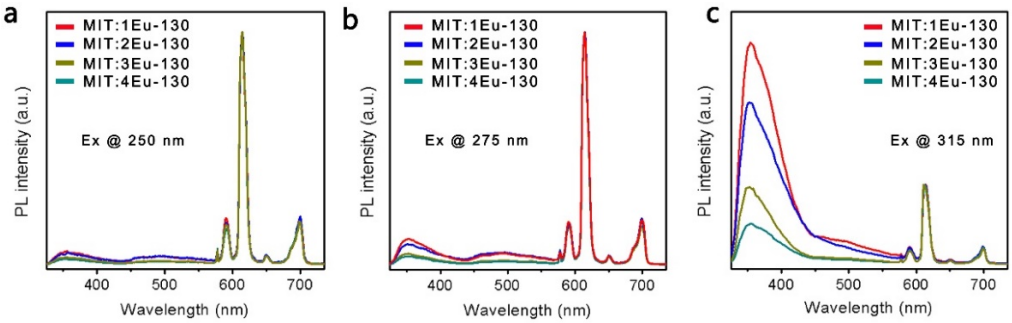

Figure S18. Normalized steady-state emission spectra of MIT:Eu-130 with different europium contents excited at (a) 250 nm, (b) 275 nm, and (c) 315 nm under ambient conditions. The spectra were normalized to the intensity of band M at 614 nm.

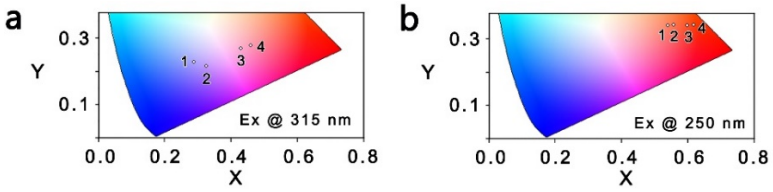

Figure S19. CIE coordinate diagrams of the MIT:Eu-130 samples excited at (a) 315 and (b) 250 nm, respectively. Labels “1, 2, 3, 4” correspond to MIT:1Eu-130, MIT:2Eu-130, MIT:3Eu-130, and MIT:4Eu-130, respectively.

Table S11. CIE chromaticity coordinates for MIT:Eu-130 with different europium content.

Excitation 250 nm		Excitation 315 nm	
Sample	CIE coordinates (x, y)	Sample	CIE coordinates (x, y)
MIT:1Eu-130	(0.540, 0.340)	MIT:1Eu-130	(0.289, 0.228)
MIT:2Eu-130	(0.558, 0.341)	MIT:2Eu-130	(0.325 0.215)
MIT:3Eu-130	(0.599, 0.339)	MIT:3Eu-130	(0.429, 0.267)
MIT:4Eu-130	(0.618, 0.340)	MIT:4Eu-130	(0.459, 0.278)

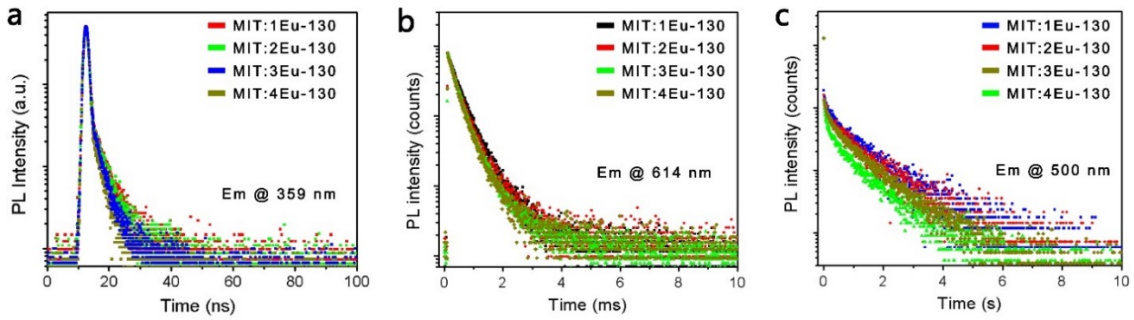

Figure S20. Luminescence decay profiles of dehydrated MIT:Eu-130 samples with different europium content monitored at (a) 359 nm, (b) 614 nm, and (c) 500 nm under ambient conditions.

Table S12. Fitting results of the decay curves of dehydrated MIT:Eu under ambient conditions.

Samples	Emission wavelength (nm)	*A* (%)	τ (ns)	τ (us)	τ (s)	R^2
MIT:1Eu-130	359	100	2.82	-	-	0.983
MIT:2Eu-130	359	100	2.80	-	-	0.987
MIT:3Eu-130	359	100	2.76	-	-	0.972
MIT:4Eu-130	359	100	2.73	-	-	0.987
MIT:1Eu-130	614	100	-	0.365	-	0.995
MIT:2Eu-130	614	100	-	0.381	-	0.994
MIT:3Eu-130	614	100	-	0.422	-	0.997
MIT:4Eu-130	614	100	-	0.446	-	0.997
MIT:1Eu-130	500	100	-	-	1.05	0.966
MIT:2Eu-130	500	100	-	-	0.93	0.963
MIT:3Eu-130	500	100	-	-	0.79	0.979
MIT:4Eu-130	500	100	-	-	0.74	0.988

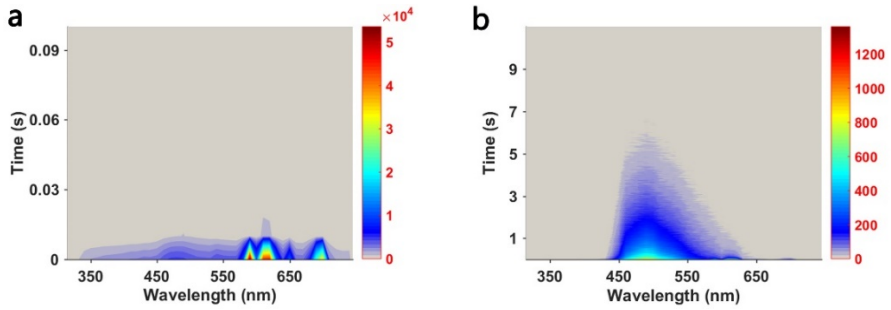

Figure S21. Time-resolved emission mapping of MIT:3Eu-85 excited at 250 nm under ambient conditions in the time range (a) from 0 to 0.1 s and (b) from 0.1 to 10 s. The color bar changing red to gray indicates the decrease in emission intensity.

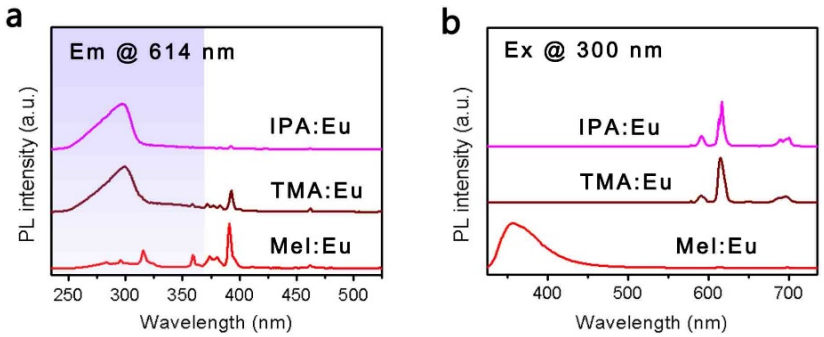

Figure S22. Normalized steady-state (a) excitation and (b) emission spectra of MeI:Eu, IPA:Eu, and TMA:Eu under ambient conditions.

Supplementary References

1. L. Bian, H. Shi, X. Wang, K. Ling, H. Ma, M. Li, Z. Cheng, C. Ma, S. Cai, Q. Wu, N. Gan, X. Xu, Z. An and W. Huang, *Journal of the American Chemical Society*, 2018, **140**, 10734-10739.
2. E. R. Souza, I. G. Silva, E. E. Teotonio, M. C. Felinto and H. F. Brito, *Journal of luminescence*, 2010, **130**, 283-291.
3. H. Zhang, L. Zhou, J. Wei, Z. Li, P. Lin and S. Du, *Journal of Materials Chemistry*, 2012, **22**, 21210-21217.
4. M. Hasegawa, A. Ishii, K. Habu, H. Ichikawa, K. Maeda, S. Kishi and Y. Shigesato, *Science and Technology of Advanced Materials*, 2006, **7**, 72-76.
5. J. Saldo, E. Sendra and B. Guamis, *Innovative Food Science & Emerging Technologies*, 2002, **3**, 203-207.
6. E. Kozlovskaya, G. Pitsevich, A. E. Malevich, O. Doroshenko, V. Pogorelov, I. Y. Doroshenko, V. Balevicius, V. Sablinskas and A. Kamnev, *Spectrochimica Acta Part A: Molecular and Biomolecular Spectroscopy*, 2018, **196**, 406-412.
7. R. Bhatt, B. Sreedhar and P. Padmaja, *International Journal of Biological Macromolecules*, 2017, **104**, 1254-1266.
8. C. Yang, K. Folens, G. Du Laing, F. Artizzu and R. Van Deun, *Advanced Functional Materials*, 2020, **30**, 2003656.